

Progress in Development of Li,Be,Na/F Molten Salt Actinide Recycler & Transmuter Concept

Victor Ignatiev, Olga Feynberg, Ivan Gnidoi, Aleksandr Merzlyakov, Vladimir Smirnov,
Aleksandr Surenkov, Igor Tretiakov, Raul Zakirov
Russian Research Center – Kurchatov Institute, Moscow, RF
Valery Afonichkin, Andrei Bovet
Institute of High Temperature Electrochemistry, Ekaterinburg, RF
Vladimir Subbotin, Aleksandr Panov, Andrei Toropov, Alexei Zherebtsov
Institute of Technical Physics, Snezhinsk, RF
Tel. +7-495-196-71-30, Fax. +7-495-196-86-79, E-mail: ignatiev@quest.net.kiae.su

Abstract –*To examine and demonstrate the feasibility of molten salt reactors to reduce long lived waste toxicity and to produce efficiently electricity in closed fuel cycle some national and international studies were initiated last years. In this paper main focus is placed on experimental and theoretical evaluation of single stream MOLten Salt Actinide Recycler & Transmuter (MOSART) system fuelled with compositions of plutonium plus minor actinide trifluorides (AnF_3) from PWR spent fuel without U-Th support. The paper summarizes the most current status of the MOSART design data received within ISTC#1606 phase 2.*

I. INTRODUCTION

Recent years have demonstrated a growing interest in the nuclear energy systems employing the technology of molten salt fluorides. Among the systems selected in GIF Generation IV, Molten Salt Reactors (MSR) presents a promising flexible option in response to the goals and criteria assigned to future nuclear systems: fuel cycle sustainability, safety, environmental impact, proliferation resistance, diversity of applications and economics.

A study is underway within ISTC#1606 phase 2 to examine and demonstrate the feasibility of MOLten Salt Actinide Recycler & Transmuter (MOSART) system to reduce long lived waste toxicity and to produce efficiently electricity in closed cycle.¹⁻³ Focus is placed on the experimental and theoretical evaluation of single stream MOSART concept fuelled with different compositions of plutonium and minor actinides from LWR spent fuel without U-Th support.

These studies are performed in the following main work packages:

1. Study on system's neutronic, thermal hydraulic and fuel cycle properties, accounting for technology constrains.

2. Experimental consideration of fuel salt key physical & chemical properties
3. Experimental verification of Ni-Mo alloys for fuel circuit in corrosion facilities with redox measurement

As result of ISTC#1606 Phase 1 studies claim was made, that the solvent system selected appear to resolve main reactor physics, thermal hydraulics, fuel salt clean up and safety problems as applied to the Li,Be,Na/F MOSART concept¹.

This paper summarizes the most current status of the MOSART design data received within ISTC#1606 phase 2.

II. DESIGN CONSIDERATION

Design basic objective for MOSART concept is to provide the fissile concentration and geometry of the fuel salt to obtain heat release of about 2400 MWt at conditions affording the effective transmutation of plutonium and minor actinides from LWR spent fuel without U-Th support.

The fuel and coolant salts, graphite and Ni-Mo alloy are special materials for MOSART, which have been studied and developed at first in ORNL^{4,5}, later RRC-Kurchatov Institute and now under consideration within ISTC#1606^{4,5}. Principal design data for MOSART fuel

circuit received in our study are given in Tables I and II. Plan view of MOSART fuel circuit is shown on Fig. 1.

There is, of course, not one possible arrangement of MOSART unit. Fig. 1 shows the preliminary primary system design configuration that is used to evaluate its neutronics and thermal hydraulics feasibility. As in well-established MSBR⁴ design the fluoride fuel salt mixture is circulated through the reactor core by four pumps operating in parallel. Pumps circulate salt through heat exchangers and return it to a common plenum at the bottom of the reactor vessel. Each circuit contains a 1 m³/s single stage centrifugal pump and a shell-and-tube heat exchanger.

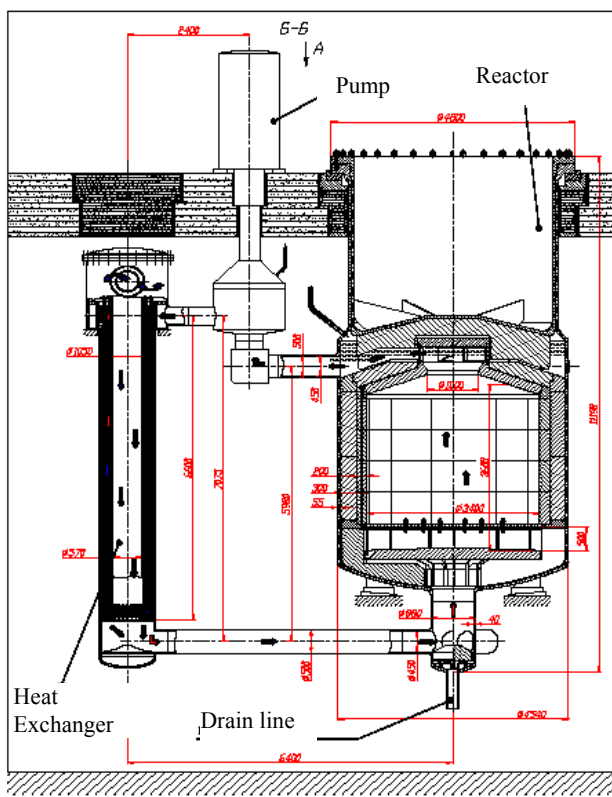


Fig. 1: MOSART Fuel Circuit

Heat is transferred from the primary salt to secondary fluid NaF-NaBF₄ having composition 8-92 mole % and liquidus temperature 384°C. Each of the four secondary circuits has a 1.3 m³/s centrifugal pump with variable-speed drive. In addition to its primary functions of isolating the highly radioactive primary circuit from the steam system and serving as an intermediate heat transfer fluid, the molten NaF-NaBF₄ mixture would play a major role in limiting the release of tritium from MOSART system.

Tritium, xenon and krypton are sparged from circulating fuel salt by helium introduced in a side stream

by a bubble generator and subsequently removed by a gas separator. Provisions are made for maintaining soluble fission products at low required level by fuel salt processing. To minimize actinide losses in reprocessing we considered removal time about 300 edpf for soluble fission products (rare-earth trifluorides). The reactor is capable of being drained essentially free of salt and afterheat following shutdown can be safely dissipated.

TABLE I
 Principal Design Data

	MOSART	MSBR
Thermal capacity, MWt	2400	2250
Reactor vessel ID, m	4.54	4.43
Vessel wall thickness, cm	5.5	5.1
Vessel design pressure, N/m ²	5.2·10 ⁵	5.2·10 ⁵
Core height, m	3.6	3.96
Radial thickness of reflector, cm	20	76.2
Volume fraction of salt in core, %	100	13/37
Average core power density, MW/m ³	75.0	22.2
Peak core power density, MW/m ³	163	70.4
Average neutron flux, n·cm ⁻² ·s ⁻¹	10 ¹⁵	2.6·10 ¹⁴
Max graphite damage flux, n·cm ⁻² ·s ⁻¹	1.45·10 ¹⁴	3.3·10 ¹⁴
Graphite temperature at max graphite damage region, K	1084	982
Estimated useful life of graphite, yrs	4	4
Total weight of graphite, t	20	304
Average salt velocity in core, m/s	0.5	1.3
Total fuel salt in reactor vessel, m ³	40.4	30.4
Total fuel salt in primary system, m ³	56.2	48.7
Cycle time for salt inventory, efpd	300	30

The start up and feed fuel material scenarios for MOSART critical core are following: 1) TRU from UOX spent fuel of a commercial PWR (60 GWd/tU - 4.9% ²³⁵U/U; after 1 year cooling); 2) 4.9% ²³⁵U/U irradiated in PWR up to 60 GWd/tHM (Stage 1); after 7 years cooling the Pu from the spent fuel it is used for MOX fuel production with natural uranium and 7% Pu; after 3 additional years of MOX fuel production, this fuel also irradiated in PWR up to 60 GWd/tHM (Stage 2). Remained Pu and minor actinides from Stage 1 irradiation, after 10 years cooling are the fuel for MOSART.

Fuel salt is molten 15LiF-27BeF₂-58NaF (in mole%) mixture with 479°C melting temperature fuelled by trifluorides of actinides with mass proportion at equilibrium for chosen fuel cycle scenario. Lithium is enriched to 99.99% ⁷Li. In the design of the MOSART, the material that is specified for nearly all metal surfaces contacting the fuel and coolant salts is an alloy, which is modification of the present commercial Hastelloy N (see Section III). The only exception is part of the chemical

processing system, which are made of molybdenum, and the infrequently used fuel storage tank, which is of stainless steel.

2400MWt MOSART system has the cylindrical core having an intermediate to fast energy spectrum of neutrons. No solid material is present in the core of this reactor as moderator. The salt inlet temperature in core is assumed as 600°C. The diameter / height of the cylindrical core is about 3.4 m / 3.6 m. The effective flux of such system is near $1 \cdot 10^{15} \text{ n cm}^{-2} \text{ s}^{-1}$. Fuel salt specific power is about 43 W/cm³. The core salt mass flow rate is 10000 kg/s. Average axial velocity of stream in core is equal about 0.5m/s. The fuel salt enters the core through inlet radial window at the bottom of core and the salt flow is upward through the core to promote natural circulation. The fuel salt leaves the reactor vessel through outlet pipe attached to the top reflector. Out core circulation time is about 4 s.

TABLE II
 Characteristics of Heat Exchangers

	MOSART	MSBR ²
Inlet/outlet fuel salt temperature, K	873/988	839/978
Fuel salt mass flow rate, kg/s	10000	11820
Secondary salt mass flow rate, kg/s	9400	8872
Fuel salt velocity, m/s	5	3
Tube spacing in heat exchanger on pitch circle, mm	12.2	18.8
ID of central tube in heat exchanger, m	0.57	0.51
Shell ID, m	1.05	1.73
Tube OD, mm	10	9.5
Total number of tubes in four heat exchangers	18591	23584
Length of one heat exchanger, m	6.6	6.8
Total volume of fuel salt in heat exchangers tubes, m ³	6.2	7.6
Heat transfer coefficient, primary side, W/m ²	17100	-
Heat transfer coefficient, secondary side, W/m ²	17656	-
Overall heat transfer coefficient, W/m ²	5700	4820
Pressure drop in heat exchanger, primary side, kPa	660	890

For MOSART graphite reflector there is no strong requirement on gas permeability ($10^{-8} \text{ cm}^2/\text{s}$), but molten salt should be excluded from the open pore volume (pore structure < 10^{-6} m). Last requirement can be met by currently available commercial graphite. Optimal thickness for removable radial and axial graphite reflectors accounts for 0.2 m. Cooling was provided for the reactor vessel and other parts of design to keep temperatures within the tolerances imposed by neutron fluence and stress conditions. About 1% of the reflector volume is the fuel salt. Owing to relative power in graphite reflectors the total

fuel salt flow rate through reflectors was chosen 275 kg /s (2.75 % from the total flow). Neutron fluences and maximum graphite temperatures are kept low enough to provide an estimated reflector graphite life of about four years. Thermal conductivity and density of the graphite reflectors was accepted equal to the following values: $\lambda_c = 57 \text{ W} \cdot \text{m}^{-1} \cdot \text{K}^{-1}$ and $\rho_c = 1800 \text{ kg/m}^3$.

Between reflector and reactor vessel, 30 cm width steel blocks with 1% of fuel salt are installed to reduce the damage flux arriving at surface of the 5cm reactor vessel wall made of Ni- Mo alloy. To minimize the reactor vessel wall temperature the 5mm fuel salt annulus is assumed between iron blocks and reactor vessel.

The reactor vessel is about 4.54m in diameter and 11.2 m high. It has 55mm thick walls and 75 mm –thick dished heads at the top and bottom. The 15 cm diameter fuel salt drain line connects to the bottom of the reactor vessel inlet manifold. The reactor vessel is expected to last of the life of the plant. The reactor is capable of being drained essentially free of salt and afterheat following shutdown can be safely dissipated.

III. CORE NEUTRONICS, THERMAL HYDRAULICS AND FUEL CYCLE

The equilibrium fuel salt composition was obtained with the help of MCNP-4B+ORIGEN2.1 code (with library received on the basis of ENDF/B-V,VI) calculation of transition to equilibrium of 2400MWt MOSART core with soluble fission product removal time equal 300 efpd.

For 2400MWt homogeneous cylindrical core with 20cm nickel and graphite reflectors at equilibrium critical loading 3D power distribution maps have been obtained. Differ from Ni reflector for graphite one there is the power growth (up to 60% from the maximal value in the core centre) on the boundary of the fuel salt and graphite reflector due to thermal neutrons return to the core. The total power outputs due to n+γ radiation for the graphite and nickel reflectors have been obtained. The relative power in graphite and nickel reflectors are 2.2% and 1.7% of total core power respectively.

On the basis of 3D power distributions received in neutronics calculations for cores with reflectors the thermal hydraulic calculations have been carried out. Calculations were executed by Russian commercial code Flow Vision. Various possibilities of fuel salt inlet / outlet for core cylindrical geometry with fuel salt cooled reflectors have been analyzed. The expediency of use of reflectors of porous type was shown.

Calculations of the coupled thermal hydraulics task (fluid convection in core with thermal conductivity in reflectors) have allowed (1) due to increase of height of radial fuel salt inlet window from 0.1 m up to 0.5 m and (2) using top conic reflector, instead of a flat one, to carry out alignment of core velocity distribution. Alignment of a velocity distribution has resulted in significant reduction of the maximal fuel salt temperature in core from 1385K down to 1107K. The peak temperature of a radial reflector has made 1142K, in the bottom and top reflector - accordingly 1098K and 1085K. However in the bottom part on periphery of core small recirculation area was kept.

Introduction of the distribution plate at core inlet with porosity of 32 % has allowed completely to avoid recirculation areas of flow and to lower the maximal temperature of fuel salt to a level 1034K, that only 46K higher than average fuel salt temperature at core outlet. The maximal temperature of radial nickel reflector has made 1119K, of bottom and top reflectors - accordingly 1096K and 1063K.

Transition to graphite reflector for given power distributions essentially has not changed significantly the characteristic (velocity and temperature distributions of fuel salt) in core and reflectors. The maximal temperature in core has increased on 2K and has made 1036K. The temperature of a radial reflector has decreased in comparison with similar variant with a nickel reflector from 1119K down to 1087K, temperatures of the bottom and top reflectors have decreased on 10K and 20K accordingly.

The optimized MOSART core configuration satisfies the two most important thermal hydraulic considerations: (1) the maximum temperature of solid reflectors is low enough to allow it use for suitable time and (2) regions of reverse or stagnant flow are avoided.

Further specification of thermal hydraulics characteristics of core and reflectors may be received by use of two-temperature model of a porous body. Also it will be necessary to take into account reactor vessel protection required, by e.g. 30 cm width iron blocks with 1% of fuel salt installed to reduce the damage flux arriving at surface of the reactor vessel wall made of Ni-Mo based alloy. To minimize the reactor vessel wall temperature the 5mm fuel salt annulus would be assumed between iron blocks and reactor vessel.

Received on a thermal hydraulic stage of calculation the improvement of MOSART core design and 3D temperatures distributions of the core and reflectors were used for specification of system neutronic characteristics (see Fig. 2 and 3). As can see from Fig. 2 for last core

configuration the required AnF_3 concentrations in fuel salt for equilibrium critical loadings, as for the scenario 1 (1.03 mole%, compared to 0.6 mole% for infinite core) and for the scenario 2 (1.30 mole% compared to 0.8 mole% for infinite core), remain truly less than trifluorides solubility limit (2 mole%) for chosen carrier salt at minimal temperature in primary circuit 600 °C, even in view of probable uncertainties in the neutron cross-sections of minor actinides. Contribution to the system's neutron balance of the nuclides up to ^{251}Cf was considered. Note, that at equilibrium, AnF_3 concentration (in mole%) is about one order of magnitude higher than that of LnF_3 in fuel salt. Transient to equilibrium in 2400MWt MOSART core needs about ten years. Masses of plutonium and minor actinides in primary circuit at equilibrium according MCNP calculation for scenario 1 and scenario 2 are respectively 7320 kg and 9346 kg.

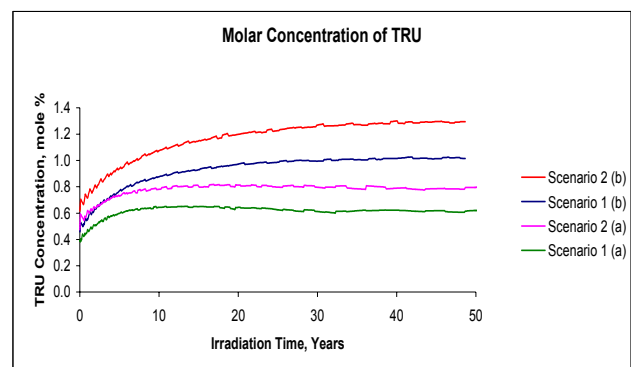


Fig. 2 Fissile AnF_3 concentrations for different MOSART start-up and feed fuel salt compositions at transient to equilibrium: a-infinite in radial direction core, b-finite core.

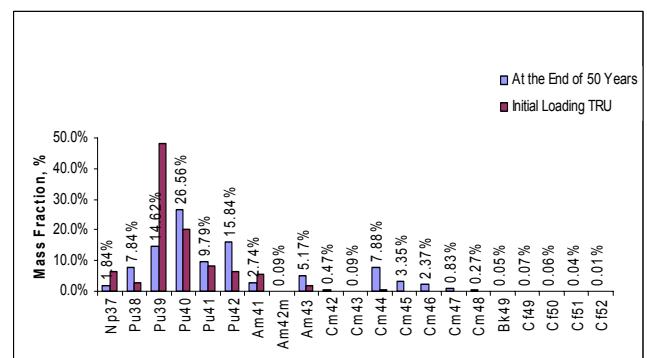


Fig. 3. Actinides mass fraction in MOSART: Scenario 2

Data obtained as a result of the burn up calculations permit to determine integral parameter, characterizing system efficiency for plutonium and minor actinides transmutation:

$$K_G(t) = \frac{N_F^{TRU}(t)}{N^{TRU}(t)},$$

where $N^{TRU}(t)$, and $N_F^{TRU}(t)$ -full amount, respectively, loaded and burned plutonium plus minor actinides during period t (this parameter is proportional to the core thermal power and reaches its maximum in critical system of MOSART type fuelled by only plutonium and minor actinides).

If we deal with the critical system loaded by only plutonium and minor actinides with relatively small transition to equilibrium time:

$$\frac{1}{K_G(T)} = 1 + \frac{M_E}{P} E_f \left(\frac{z}{\tau} + \frac{1}{T} \right),$$

where T -lifetime of the fuel loading, M_E -equilibrium plutonium and minor actinides loading, P - thermal power of the system, E_f - fission energy, $1/\tau_i$ - soluble fission product removal rate; z_i - losses to waste.

As can see K_G aspires to maximal meaning for the systems with long lifetime T , minimal possible equilibrium specific loading (M_E/P) and minimal losses to waste in fission products removal process (z/τ). For the case of actinides losses to waste stream in single pass $z=10^{-3}$ and $T=50$ yrs K_G factor responsible for transmutation efficiency and equal 0.95 for the infinite in radial direction core loaded by scenario 1 is decreased for the case of 3D finite core down to 0.83. For scenario 2 last value is equal 0.80.

The experimental data on fuel salt density obtained (see next Section) have been used for calculation of temperature reactivity coefficients in 2400MWt MOSART core with 0.2m graphite reflector for the equilibrium critical fuel loading in the temperature range 900 – 1600K. Calculations have been done in assumption of core isothermal fuel salt temperature and on base of 3D temperature distributions for core operating at nominal power, received in thermal hydraulic calculation. The account of temperatures distribution in the core operating at nominal power, make temperature reactivity coefficients more negative, compared to isothermal core. For last case they are equal to -4.125 pcm/K and -6.625 pcm/K for the first and the second scenarios of the equilibrium critical loading, respectively.

Within IAEA coordinated research “Studies of Innovative Reactor Technology Options for Effective Incineration of Radioactive Waste” the comparison of 2400MWt MOSART core neutronic characteristics (for scenario 1) by different calculation schemes was carried out³. The received results have confirmed essential

distinction in cross-sections of minor actinides used in different libraries. At the same time the results obtained with the help of different codes, but with the use of the same nuclear data coincide rather well. The disorder in values of K -eff is near 2.5 %. Thus the maximal value gives JEFF3.1, and minimal ENDF6.8.

Work on comparison of neutronic, thermal hydraulic and safety related parameters of MOSART core, obtained by different calculation schemes with attraction of new results will be continued.

Fig. 4 shows preliminary conceptual flow sheet for MOSART fission products clean up unit. Most important processing operations consist in recycling of actinides for transmutation and removal of lanthanides in order to hold actinides plus lanthanides concentration in the fuel salt below the solubility limit and neutron absorption in lanthanides to acceptable level.

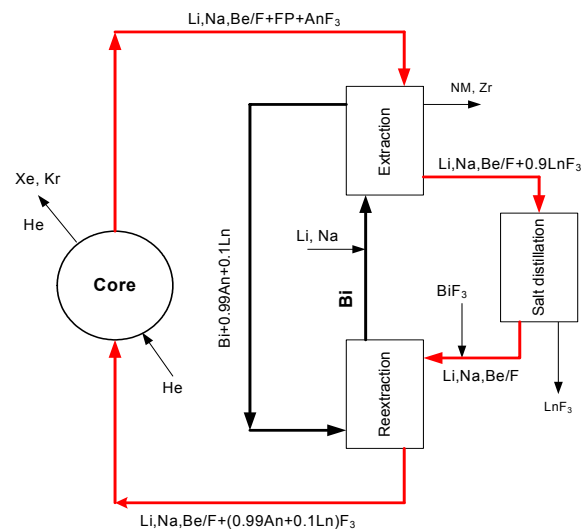


Fig. 4. Conceptual scheme of MOSART fuel salt clean up

At the first stage of the fuel salt clean up all actinides and some of fission products (noble metals, zirconium) are co-extracted into liquid bismuth. At the second stage lanthanides are separated from the $Li, Be, Na/F$ solvent by method of salt distillation. This method of lanthanides removal is under consideration, because our last experiments indicate that in lanthanides extraction process the large amount of sodium is removed into liquid bismuth from $Li, Be, Na/F$ system. Further, the actinides are re-extracted and recycled to the core for transmutation. Sodium extraction could be sufficiently decreased by sodium addition into liquid bismuth.

The $Li, Be, Na/F$ salt distillation process could produce some problems, because of high temperatures (1200-1300⁰C) needed to achieve necessary distillation capacity

(about 0.2 m³ per day). However, these difficulties would be managed. For example, the amount of salt distilled could be sufficiently decreased by preliminary crystallization of the main part of lanthanides in cold traps.

IV. PHYSICAL AND ELECTROCHEMICAL PROPERTIES OF FUEL SALT.

IV.A. Physical Properties

Below are listed the main physical properties of molten 15LiF-27BeF₂-58NaF (mole %) and 17LiF-58NaF-25BeF₂ (mole%) mixtures received to be used in the design calculation:

Composition 15LiF-27BeF₂-58NaF (mole %) corresponds to ternary eutectic with liquidus temperature 479±2°C. Liquidus temperature was determined using curves of heating and for composition 17LiF-25BeF₂ - 58NaF (mole%) is equal to 486±2°C.

PuF₃ solubility in the melt was measured by original technique of local γ -spectrometry. It provides reliable determination of equilibrium in system melt-solid state and measurement with relative error less than 9%. For molten 17LiF-25BeF₂-58NaF and 15LiF-27BeF₂-58NaF mixtures (in mole %), the data appear to follow a linear relationship within the experimental accuracy of the measurements when plotted as $\ln P$ of molar concentration of PuF₃ vs. 1/T(K), respectively:

$$\ln P = -0,6334 \cdot \frac{10^4}{T} + 8,38$$

$$\ln P = -0,5936 \cdot \frac{10^4}{T} + 7,49$$

For molten 15LiF-58NaF-27BeF₂ and 17LiF-58NaF-25BeF₂ (mole%) mixtures the following solubility of PuF₃ was obtained in our study: 1.33 and 1.94 mole % at 550°C and 1.94 and 3.00 mole % at 600°C. The effect of NdF₃ on the solubility of PuF₃ in molten 17LiF-25BeF₂-58NaF (mole %) mixture was determined. Presence of EuF₂ up to 0.3 mole % in solvent did not affect PuF₃ solubility in molten 17LiF-25BeF₂-58NaF (mole %) mixture.

Density of the melts has been measured by hydrostatic weighting method in temperature range 482 - 770 °C. The mistake of measurement is estimated as 0.9 %. The following correlation of density on temperature of molten 15LiF-58NaF-27BeF₂ and 17LiF-58NaF-25BeF₂ (mole%) mixtures are obtained respectively:

$$\rho [g/cm^3] = 2.163 \pm 0.0023 - (4.06 \pm 0.29) 10^{-4} (t[^\circ C] - 601.4)$$

$$\rho [g/cm^3] = 2.150 \pm 0.0029 - (3.34 \pm 0.44) 10^{-4} (t[^\circ C] - 678.5)$$

Analysis of experimental data shows, that for molten 15LiF-27BeF₂-58NaF (mole%) mixture value (-4.06±0.29) 10⁻⁴ [g/(cm³K)] can be recommended for factor $d\rho/dt$. Processing of experimental data for 17LiF-58NaF-25BeF₂ gives value $d\rho/dt = (-3.34 \pm 0.44) 10^{-4}$ [g/(cm³K)].

Thermal conductivity of molten Li,Be,Na/F system has been measured by monotonous heating technique in temperatures range 500-750°C. Total dispersion of measurements is determined by accuracy of calibration and estimated as 15 %. The following correlation are obtained by least squares method:

$$\lambda (W/(m K)) = 0.838 + 0.0009 [t (^\circ C) - 610.3]$$

Viscosity of different molten Li,Be,Na/F mixtures have been measured by method of attenuation torsional oscillations of the cylinder with melt under study in a temperature range from freezing up to 800°C. Accuracy of measurement is 4-6 % (dispersion). Dependence of 15LiF-27BeF₂-58NaF (mole %) mixture kinematic viscosity vs temperature in the temperature range 480 - 800 °C is represented as:

$$\nu (m^2/s) = 0.1360 \exp\{2914/T(K)\}$$

Addition to molten 15LiF-27BeF₂-58NaF (mole %) mixture of 1 mole % CeF₃ (as PuF₃ proxy) leads to some decrease of kinematic viscosity. This effect is negligible at high temperatures, and grows up to 25-30% at temperature decreasing down to 550°C.

Heat capacity for temperature range from 700 to 1000 K was evaluated basing on data molten for binary systems and individual components: $C_p = 2090 J \cdot kg^{-1} \cdot K^{-1}$.

Vapor pressure (in Pa) was evaluated by ideal mixture method basing on data molten for binary systems and individual components:

$$\ln p = 18.920 - 1.469 \cdot 10^{-4} T(K) - 25283/T + 0.9819 \ln(T).$$

IV.B. Electrochemical Properties

The electrochemical behavior of PuF₃, NdF₃ and ZrF₄ solutions in 15LiF-58NaF-27BeF₂ and 60LiF-40NaF (mole %) melts were studied by cyclic voltammetry (CV) with linear potential sweep and chronopotentiometry methods. 60LiF-40NaF (in mole %) melt was investigated as possible alternative solute for electrochemical separation of actinides and lanthanides. The concentration of PuF₃ in fluoride melts investigated was equal $(0.3-1) \cdot 10^{-5}$ mole/cm³.

The main results of the experiments carried out:

- In 15LiF-58NaF-27BeF₂ melt plutonium is deposited on molybdenum cathode earlier than beryllium;
- Difference of deposition potentials of plutonium and beryllium in 15LiF-58NaF-27BeF₂ melt is equal $\Delta E_{\text{Pu-Be}} = 0.15 \pm 0.02$ V (913K) and for plutonium and neodymium this value is estimated as $\Delta E_{\text{Pu-Nd}} \approx 0.3$ V;
- Difference of deposition potentials of Pu and Na in 60LiF-40NaF is equal $\Delta E_{\text{Pu-Na}} = 0.30 \pm 0.02$ V (1023K);
- Deposition potentials of Nd in 60LiF-40NaF melt containing NdF₃ is more negative than deposition potential of sodium; therefore Na is deposited on solid Mo working electrode (WE).

CVs of 15LiF-58NaF-27BeF₂ and 60LiF-40NaF (mole %) melts with PuF₃ addition are presented in Fig. 5 and 6.

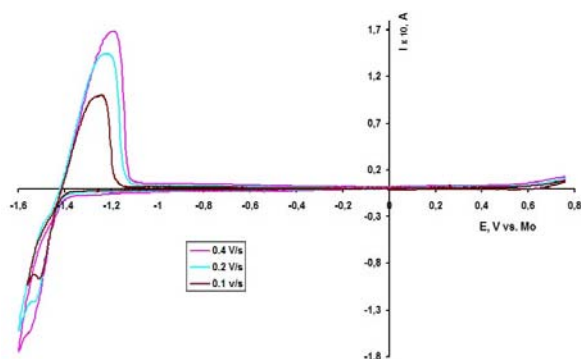


Fig. 5. CV of PuF₃ ($5 \cdot 10^{-5}$ mole/cm³) in 15LiF-27BeF₂-58NaF melt for various scan rate. WE - Mo ($S \approx 0.5$ cm²), RE - Mo. T=853K.

Equilibrium electrode potentials of Pu³⁺/Pu⁰ and Be²⁺/Be⁰ couples in 15LiF-27BeF₂-58NaF and Pu³⁺/Pu⁰ and Na⁺/Na⁰ couples in 60LiF-40NaF (mole%) melts are equal:

$$E_{\text{Pu}^{3+}/\text{Pu}^0} \approx -1.75 \pm 0.05 \text{ V (Na, Li, Be/F; 893K)}$$

$$E_{\text{Be}^{2+}/\text{Be}^0} = -1.90 \pm 0.01 \text{ V (Na, Li, Be/F; 893K)}$$

$$E_{\text{Pu}^{3+}/\text{Pu}^0} \approx -1.63 \pm 0.02 \text{ V (Na, Li/F; 1023K)}$$

$$E_{\text{Nd}^{3+}/\text{Nd}} < E_{\text{Na}^+/\text{Na}} = -1.93 \pm 0.01 \text{ V (Na, Li/F; 1023K)}$$

Equilibrium electrode potentials were measured with respect to reference electrode (RE) based on Ni/NiF₂ (redox couple Ni²⁺/Ni⁰, 1 mole % NiF₂ in fluoride melts). The behavior of the reference electrode used was not stable. For this reason it is necessary to regard these equilibrium electrode potential values as assessed values. A value of the diffusion coefficient of Pu³⁺ ions in the 15LiF-58NaF-27BeF₂ melt with addition of PuF₃ ($9 \cdot 10^{-5}$ mole/cm³) calculated using the Randles-Sevcik equation is equal $D_{\text{Pu}^{3+}} \approx 5 \cdot 10^{-5}$ cm²/s (T=893K).

An assumption was made concerning the alloying of plutonium with Be and Ni in the process of plutonium ions electrochemical reduction in fluoride melts under investigation. Based on the experimental results received it is possible to assert, that electrowinning on solid cathodes could be used for fuel salt clean up from corrosion products and for An/Ln separation. Further studies are necessary in order to determine the nature of Pu-Ni alloying and its utilization in the process of plutonium recovering from fuel salt.

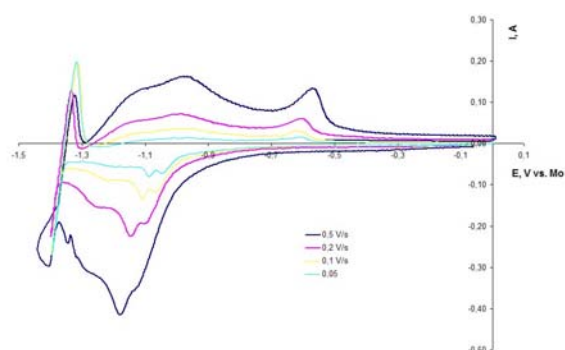


Fig. 6. CV of PuF₃ ($3.1 \cdot 10^{-5}$ mole/cm³) in LiF-NaF melt for $v = 0.05, 0.1, 0.2, 0.5$ V/s. WE - Mo ($S \approx 0.4$ cm²), RE - Mo. T=1023K.

IV.C. Validation of Ni|NiF₂ Reference Electrode

The emf method and cyclic voltammetry were used to study different electrochemical cells with a nickel RE placed in a graphite container having an insulating PBN coating. A bridge of the salt melt in a capillary 0.1 mm diameter provided the ionic conduction. The conditional standard potentials of sodium and beryllium were evaluated at temperatures of 800 to 1000 K. The thermodynamic functions ΔH^* , ΔS^* and ΔG^* of oxidation reactions of sodium and beryllium by NiF₂ solutions in the 17LiF-25BeF₂-58NaF (mole%) melt were calculated.

It was found that NiF₂ solutions in molten 60LiF-40NaF and 17LiF-25BeF₂-58NaF mixtures were very sensitive to changes of the composition and redox potential of the environment (the gaseous atmosphere, the test melt). As a result, a nickel powder or nickel films were formed on the container walls, in the bulk and on the surface of the melt during long-term experiments. The decrease in the NiF₂ concentration of the RE standard melt led to an uncontrolled drift of the RE potential and erroneous measurement of the emf. Precipitation of metallic nickel from the melt caused plating of the RE capillary and appearance of the electron conduction on the walls of the salt bridge. Ultimately, a short circuit occurred between the half-elements of the electrochemical cell.

The thermodynamic simulation of the reactions taking place in the systems under study suggested that at the experimental temperatures PBN interacted with NiF_2 solutions by an endothermic reaction, which was followed by the formation of nickel, NaBF_4 and nitrogen (Fig.7). As a result, the PBN insulator lifetime on the surface of RE graphite container is limited and decreases with growing temperature.

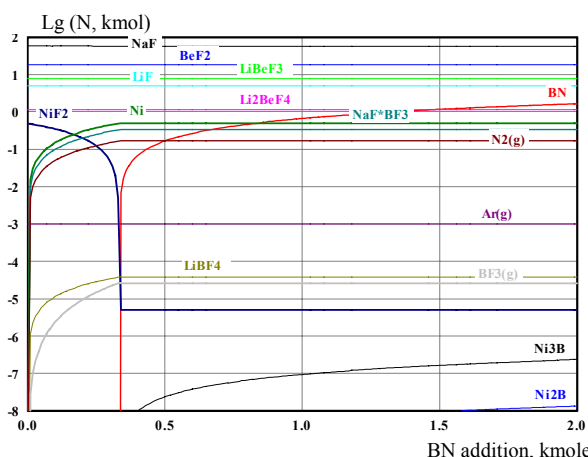


Fig. 7. Variation of the assigned equilibrium composition of the initial reaction mixture (17LiF-25BeF₂-58NaF) + 0.5 mole % NiF₂ when additions of boron nitride were introduced in sequence at 500 °C.

Advances in the development of a simple reliable nickel RE are possible, if following R&D will be performed:

- Development of designs providing isolation of the nickel RE from the cell atmosphere and preventing the direct contact of salt melts with the NiF_2 solution in the RE half-element;
- Selection of up-to-date solid electrolytes and inert insulating materials for solid ion conducting membranes, which would preserve their properties over a wide interval of the redox potential of the fluoride salt melt;
- Development of reliable methods for protection of the container and membrane materials against corrosive salt melts; the use of up-to-date coating deposition technologies for this purpose;
- Standardization of methods for production of containers with ion conducting diaphragms (membranes)

V. MATERIALS COMPATIBILITY

ISTC#1606 corrosion task include following stages:

- Compatibility test between Ni-Mo alloys and molten 15LiF-27BeF₂-58NaF salt in natural convection loop.
- Study on PuF₃ addition effect in molten 15LiF-27BeF₂-58NaF salt on compatibility with Ni - Mo alloys.

- Te corrosion study for molten 15LiF-27BeF₂-58NaF salt and Ni-Mo alloys in stressed and unloaded conditions.

Material specimens of three Hastelloy N type modified alloys, particularly: RF HN80M-VI with 1% of Nb, RF HN80MTY with 1% of Al and MONICR (Scoda, Chez Republic) we chosen for our study in corrosion facilities⁴.

The design provides tests of the materials specimens in loop at molten salt heat up about 100°C and its flow rate up to 5 cm/s (Re >3000). This loop includes the system for redox potential measurement during corrosion studies. It is installed inside the hot cell for operations with actinides.

Results of 1200 hrs loop corrosion experiment with on-line redox potential measurement demonstrated that high temperature operations with Li,Be,Na/F salt are feasible using carefully purified molten salts and loop internals. In established interval of salt redox potential 1.25-1.33 V relative to Be reference electrode, corrosion is characterized by uniform loss of weight from a surface of samples with low rate. Under such exposure salt contained respectively less than (in mass %): Ni - 0.004; Fe -0.002; Cr- 0.002. Specimens of HN80M-VI and HN80MTY from hot leg of loop exposed at temperatures from 620°C till to 695°C showed uniform corrosion rate from 2 μm/ year to 5 μm/ year. For MONICR alloy this value was in the range of 9 - 19 μm/ year.

It was not found any significant change in corrosion behavior of materials samples in melt due to the presence of 0.5 mole % PuF₃ addition in Li,Be,Na/F salt. Specimens of HN80M-VI from the loop exposed during 400 hrs at temperature 650°C showed uniform corrosion rate of about 6 μm/ year. Under such exposure salt contained respectively about (in mass %): Ni - 0.008; Fe -0.002; Cr- 0.002. It was not found any traces of intergranular cracking for all specimens after loop tests even in the melt with PuF₃ addition. Data of chemical analysis of specimen's surface layer showed decrease of the chromium contents by the 10-20 μm.

As first step of Te corrosion study ampoule tests with Cr₃Te₄ source were done. The alloy resistance to intergranular cracking was estimated by parameter "K", which is value equal to product of cracks number on 1 cm length of longitudinal section of specimen subjected to tensile strain, multiplied by average cracks depth in μm.

The first set was made for unloaded conditions with well-purified salt reduced by metallic beryllium, and the second one – with addition of nickel difluoride. In the first set of ampoules after 100hr exposition at 650°C in 15LiF-58NaF-27BeF₂ melt containing (in mass.%) respectively: Te<0.01; Ni - 0.008; Fe -0.02; Cr< 0.001 the traces of

intergranular cracking were found only on MONICR samples ($K = 30 \text{ pc}\cdot\mu\text{m/cm}$). For the second set with melt containing (in mass.%): Te<0.01; Ni-0.26; Fe-0.0095; Cr-0.39 microphotographs showed that the surfaces of all alloys are full of cracks along the grain boundaries to the depth from $30 \mu\text{m}$ up to $60 \mu\text{m}$: MONICR ($K = 7920 \text{ pc}\cdot\mu\text{m/cm}$), HN80M-VI ($K = 3420 \text{ pc}\cdot\mu\text{m/cm}$) и HN80MTY ($K = 1040 \text{ pc}\cdot\mu\text{m/cm}$).

Studies on Te addition effects in molten $15\text{LiF}\cdot 27\text{BeF}_2\cdot 58\text{NaF}$ salt (mole%) on compatibility with Ni - based alloys both in stressed and unloaded conditions in corrosion test facility with redox potential measurement are underway now within ISTC#1606 and more new experimental results coming soon.

IV. SPECIAL MATERIALS INVENTORIES

As can see from Table III total inventory of $\text{LiF}\cdot\text{NaF}\cdot\text{BeF}_2$ in the primary system will make, approximately, 120 t (from them the reactor vessel will contain approximately 86 t of salt). Thus, for primary system is required 71.4 t NaF, 11.4 t ${}^7\text{LiF}$ (3.1t of ${}^7\text{Li}$ metal) and 37.2t BeF_2 . In case of enrichment ${}^7\text{Li}$ up to 99.99 % the cost of the salt solvent inventory will make 3 000 000 \$ at the price 170 \$/kg on ${}^7\text{LiF}$ and will increase up to 10 700 000 \$ at cost 800 \$/kg on ${}^7\text{Li}$. We shall remind, that only initial inventory of fuel salt in MSBR² demanded more than 50 t ${}^7\text{LiF}$, respectively. Thus, transition from the ${}^7\text{LiF}\cdot\text{BeF}_2$ -based salt used in MSBR, to ${}^7\text{LiF}\cdot\text{NaF}\cdot\text{BeF}_2$ mixture used in MOSART, allows essentially to decrease the cost of initial solvent inventory due to minimization of expensive ${}^7\text{Li}$ amount. Cost of the secondary coolant is accepted equal 5\$/kg. At total volume of the secondary coolant in the system 240m^3 , its cost will make near 2 300 000 \$.

MOSART reactor vessel will contain up to 20 t of the graphite reflector demanding replacement of each 4 years, and about 175t of steel shielding. For comparison, the graphite initial inventory in MSBR makes 304 t, and the central part of core is subject to replacement each 4 years. It demands the additional charge of graphite 44 t/year. Thus, after 30 years of MSBR operation at NPP will be collect about 1200 t of irradiated graphite, in comparison with 160 t for MOSART system. The total cost of graphite (at specific cost 30 \$ / kg) required 30 years MOSART operation will not exceed 5 000 000 \$.

The carried out estimations of capital making cost of MSBR included significant uncertainty because of uncertainties in design. From them, in particular, followed, that cost of primary and secondary salt carriers was insignificant compared to the total capital investments in the plant, whereas expenses for components made from Hastelloy NM (29 %) and graphite (6 %) made about 35 % from the total capital investments. In cost of

components made of Hastelloy NM cost of an alloy itself made about 33 %, and 67 % of cost concern to expenses for manufacturing of the main components of primary system. Already it is now obvious, that relative cost of a graphite reflector in MOSART capital making cost will make less than 1 % valid essentially smaller amount of a used material and less strict requirements to its gas permeability.

TABLE III
 Materials inventories MOSART and MSBR systems

	MOSART, t	MSBR, t
Fuel inventory	7.32 (9.35)*	(1.47 +68)**
${}^7\text{LiF}\cdot\text{NaF}\cdot\text{BeF}_2$	120	162
$\text{NaF}\cdot\text{NaBF}_4$	456	456
Graphite	20	304
Hastelloy NM	1280	1377
Steel	3028	2840

*) Pu and minor actinides for scenarios 1 (2), **) U+Th

The basic contribution to capital cost of MOSART, as well as in project MSBR, will bring the equipment made of alloy Hastelloy NM. As the weight and sizes of the main circulation pumps (hence, and their cost) not so strongly depend on capacity, transition from MSBR to MOSART conditions will change a situation insignificantly. Transition from the $\text{LiF}\cdot\text{BeF}_2\cdot\text{ThF}_4$ fuel salt used in MSBR to $\text{LiF}\cdot\text{NaF}\cdot\text{BeF}_2$ system, used in MOSART, will allow due to the better transport properties of last a little to improve specific heat removal (to lower metal consumption) in intermediate heat exchanger by 10 %.

The analysis allows planning a actions directed on reduction of cost for MOSART primary and secondary systems equipment. First of all, it is represented expedient instead of shell-tube heat exchanger to use plate type heat exchanger, made of fofered sheets with 1mm thickness. In such heat exchangers higher specific heat removal and cheaper sheet material allow to decrease cost considerably.

2400MWt MOSART system will demand 1280 t of Hastelloy NM for components of the primary and secondary circuits, that approximately on 100t lower, than in the MSBR. Consumption of Hastelloy NM in the primary and secondary circuits of MOSART is approximately equal. If to accept specific cost of Ni-Mo alloy chosen for MOSART 50 \$ / kg (it is in 6-8 times is higher than cost of products made of stainless steel) at mass 1280t, cost of a material of components of the primary and secondary circuits in 2400MWt MOSART system will make about 64 000 000 \$. The price of this alloy was determined roughly on the basis of ratio between the average cost of sheet and high-quality hire from Hastelloy N in conditions of US manufacture of in 1969-

1970, making then for a sheet of 22 \$ / kg, 55 \$/ kg for nozzles and covers, and 66 \$/ kg for heat exchanger tubes.²

V. CONCLUSIONS

In study main attention has been paid to single fluid Li,Be,Na/F MOSART system with design objective to provide the fissile concentration and geometry of the fuel salt to obtain heat release of about 2400 MWt at conditions affording the effective transmutation of plutonium and minor actinides from LWR spent fuel without U-Th support.

It is important that, as result our studies for molten Li,Be,Na/F system, was found quite wide range with minimal of LiF (17-15 mole%) and of BeF₂ (27-25mole%) content in the ternary composition, which provide fuel salt able to get PuF₃ solubility of 2 and 3 mole%, respectively, at 600⁰C, to keep adequate melting point (<500⁰C) and very low vapour pressure, to have good nuclear properties, low activation, suitable transport properties, to be well compatible with the materials in the system and moderately expensive.

2400MWt MOSART system has homogeneous core with intermediate - to- fast spectrum of neutrons. The fuel salt specific power is about 43 W/cm³. The effective flux of such system is near 1×10^{15} n cm⁻² s⁻¹. At equilibrium state for both scenarios of start up and feed actinides compositions and the soluble fission product removal cycle 300 epdf for cores with different reflector parameters considered, the AnF₃+LnF₃ concentration in fuel salt is truly within the solubility limit for molten 15LiF-27BeF₂-58NaF (mole %) at minimum fuel salt temperature in primary circuit of 600⁰C. Minimal AnF₃+LnF₃ critical concentrations at equilibrium were received for core with 0.2m graphite reflector.

2400MWt MOSART core of homogeneous configuration can satisfy most important neutronic and thermal-hydraulic considerations: (1) AnF₃+LnF₃ concentration in fuel salt is truly within the solubility limit of AnF₃+LnF₃ for molten 15LiF-27BeF₂-58NaF (mole %) at minimum fuel salt temperature in primary circuit of 600⁰C for both fuel cycle scenarios under consideration; (2) core with 0.2m graphite reflector in the temperature range 900–1600K has strong negative temperature reactivity coefficients (– 4.125 pcm/K and – 6.625 pcm/K for the first and the second scenarios of the equilibrium critical loading, respectively); (3) regions of reverse, stagnant or laminar flow are avoided and (4) the maximum temperature of solid reflectors is low enough to allow it use for suitable time.

Preliminary calculations of kinetic and dynamic characteristics of the MOSART system indicate that it would exhibit high levels of controllability and safety³. System would also possess inherent dynamic stability and would require only modest amounts of reactivity control capability.

Preliminary consideration of environment effects indicate that MOSART system could have attracted performance and actinides transmutation efficiency features while providing lower total materials inventories and waste compared to prior MSR designs, including MSBR (e.g., it allows significantly reduce to the order mass flows of graphite and ⁷Li enriched of 99.99 % in the design).

While a substantial R&D effort would be required to commercialize MOSART, there are no killing unresolved issues in the needed technology. The major technical uncertainties in the conceptual design are in the area of tritium confinement, fuel salt processing and behavior of some fission products.

ACKNOWLEDGMENTS

This effort is done by RRC-Kurchatov Institute (Moscow), VNIITF (Snezhinsk) and IHTE (Ekaterinburg) within ISTC#1606 Phase 2 supported by EU.

REFERENCES

1. V. V. Ignatiev e.a., "Integrated Study of Molten Li,Be,Na/F Salts for LWR Waste Burning in Accelerator Driven and Critical Systems", *Proc. of the GLOBAL'05*, Tsukuba, Japan, October, 9-13, 2005
2. R. S. Robertson, "Conceptual Design Study of a Single Fluid Molten Salt Breeder Reactor", ORNL-4541, 1971
3. V. V. Ignatiev et. al., "Progress in Integrated Study of Molten Salt Actinide Recycler & Transmuter System", *Proc. of 9th OECD/NEA IEM on Partitioning & Transmutation*, Nimes, France, September, 2006
4. V. V. Ignatiev e.a., "Experience with Alloys Compatibility with Fuel and Coolant Salts and their Application to MOSART concept", *Proc. of ICAPP'06*, Reno, USA, June, 2006
5. J.R. Engel e.a., "Conceptual Design Characteristics of DMSR with Once-through Fueling", ORNL/TM-7207, USA, 1980